

Quasi-surfaces waves under drift and diffusion mechanism in nonlinear interfaces[†]

E. Alvarado-Méndez^{a,*}, J.A. Andrade-Lucio^a, R. Rojas-Laguna^a,
J.M. Estudillo-Ayala^a, J.G. Aviña-Cervantes^b,
O.G. Ibarra-Manzano^a, and V. Vysloukh^c

^aFacultad de Ingeniería Mecánica, Eléctrica y Electrónica;

Depto. de Electrónica; Universidad de Guanajuato;

Apartado Postal 215-A, Salamanca, GTO., 36730 México

^bLAASS/CNRS Laboratoire d'Analyse et d'Architecture des Systèmes;;
7 Avenue du Colonel Roche, 31077, Toulouse, France

^cUniversidad de la Américas-Puebla, Dpto. de Física y Matemáticas,
Sta. Catarina Mártir, Cholula, Puebla, 72820, México

*email: ealvarad@salamanca.ugto.mx

Recibido el 4 de septiembre de 2003; aceptado el 1 de marzo de 2004

We study numerically and theoretically the behaviour of one-dimensional bright spatial soliton in an interface formed by a nonlinear media under drift and diffusion nonlinearities, and a linear one in the second media. The mechanism of diffusion causes self-bending effect on the soliton, and in consequence it is launched to nonlinear interface; after that the soliton is reflected to nonlinear medium and self-bending by diffusion newly launched the soliton to the interface. In consequence, a quasi-surface wave is formed. We present details about the trajectory, coefficient of saturation and energy during the dynamics of the spatial soliton.

Keywords: Nonlinear waveguides; optical solitons; photorefractive surface waves.

Estudiamos numérica y teóricamente el comportamiento de un solitón espacial brillante unidimensional en una interfase formada por un medio no lineal bajo las no linealidades de arrastre y difusión, y el otro medio lineal. El mecanismo de difusión da lugar al efecto de auto-doblamiento sobre el solitón, que en consecuencia es lanzado hacia la interfase no lineal. Posteriormente el solitón es reflejado al medio no lineal y el auto-doblamiento por difusión nuevamente lanza al soliton hacia la interfase. En consecuencia, una onda cuasi-superficial es formada. Presentamos una discusión detallada acerca de la trayectoria, del coeficiente de saturación y de la energía durante la dinámica de el solitón espacial.

Descriptores: Guías de onda no lineales; solitones ópticos; ondas superficiales fotorrefractivas.

PACS: 42.65Wi; 42.65Tg; 42.65H

1. Introduction

All optical switching has been performed on nonlinear interfaces [1-3]. Media with a nonzero nonlinearity, such as photorefractive crystal like: barium titanate, lithium niobate, SBN, and KTP which are highly promising prospective materials for creating all-optical switching, scanning, and processing devices, particularly those based on the use of spatial solitons. The first spatial solitons showed that the nonlinearity is produced by an external electric field that is slowly being screened [4,5]. The second type is the so-called screening solitons that occur in a steady state when the external field is non uniformly screened [6-10]. The third type is the photovoltaic solitons [11]. The soliton is a fundamental mode of the optical waveguide which is created in a photorefractive medium. Structures formed by intersecting waveguides *i.e.* by coherent [12-16] and incoherent [17,18] soliton collisions, are especially attractive from a practical point of view. In this context the interaction of spatial solitons with nonlinear interfaces is an important field of investigation because the interface can provide beam scanning over a wide range of angles with fine variations of the angle of incidence upon the interface. At the same time, an interface is a guiding system,

and the capture of spatial solitons may be associated with a nonlinear surface wave excitation [19].

A one-dimensional particle like model was developed by Aceves *et al.* [20] to obtain an equation of motion for the average location of the soliton. The interface serves as an effective induced potential barrier, which the particle (the soliton) can either pass or be reflected from, according to its “kinetic energy”. The height of the potential barrier is directly proportional to the intensity of the soliton, and the kinetic energy depends on the so-called soliton velocity, which is a function of the incident angle.

Afterwards the properties of total internal reflection were studied in a saturable nonlinearity, theoretically and experimentally [21]. For small incident angles (typically less than 1.25°) in SBN photorefractive crystal, it is possible to observe total internal reflection of the beam. Recently, the Goos-Hänchen shift effect was measured by Gilles *et al.* [22].

On the other hand, the self-bending process of steady-state bright spatial solitons in biased photorefractive media was investigated by Christodoulides *et al.* [23-25]. Self-bending of photorefractive solitons is caused by diffusion in photorefractive crystals and becomes an important effect when the beam size is in the range of the charge carriers dif-

fusion length. In consequence, the diffusion process introduces an asymmetric tilt in the light induced photorefractive waveguide, which in turn is expected to affect the propagation characteristics of these steady-state photorefractive solitons. As a result, when the diffusion process of these bright solitons is predicted [26], that is, the solitary beam center shifts quadratically with the propagation distance. The experimental observation of the self-bending of screening solitons have been done in SBN:60 [27-28].

In the present paper we study experimentally and numerically, the combined effects of the total internal reflection in nonlinear interfaces, and self-bending by diffusion effect. In Sec. 2, the physical model about the nonlinear interface (under diffusion and drift nonlinearity) is presented. In consequence the nonlinear Schrödinger equation (NLSE) is modified. In Sec. 3 numerical results are presented. In particular, the coefficient of diffusion describes the interaction between the nonlinear interface and the spatial soliton. In Sec. 4 the dynamics of the spatial soliton undulatory is presented. In Sec. 5 experimental results are presented. Finally the conclusion of the work is presented in Sec. 6.

2. Physical Model

The incidence of the beam toward nonlinear interface is represented in the Fig. 1. The left of the interface, one-dimensional beam is propagated under diffusion and drift nonlinear medium; the right is the linear medium. A valid approximation was assumed and that the complex amplitude satisfies the Eq. [3],

$$i \frac{\partial a}{\partial Z} = \frac{1}{2} \frac{\partial^2 a}{\partial X^2} + \frac{k_2^2 x_0^2}{n_{02}} \delta n a \tag{1}$$

where a is the amplitude of the electric field; $X = x/x_0$ is the transversal coordinate normalized; x_0 is the initial width of the beam; $Z = z/L_D$ is the propagation distance normalized; $L_D = kx_0^2$ is the diffraction length corresponding to x_0 ; $k = n_0\omega/c$ is the wave number; n_0 is the linear refraction index of the photorefractive crystal; ω is the carrier frequency.

In photorefractive media the change of the refractive index may be quasi-local, and a bright spatial soliton has been found, when there exists dependence between refraction index and intensity [24]. This mechanism is known as drift and is experimentally easy to make, with an external applied electric field ($E_0 \sim 0.1/1$ kV/cm) greater than the diffusion mechanism (0.01 Kv/cm approximately).

The diffusion effects in surface optical waves has been elegantly studied by García-Quirino *et al.* [29]. These waves can be guided along the boundary of the crystal with a metallic or a dielectric layer of a lower refractive index, or with a similar photorefractive crystal(PCR) with the opposite sign of the nonlinearity. Under the steady-state conditions of illumination (when nothing is changing with time) the space-charge electric field arising as a result of equal drift-diffusion equilibrium. To describe both drift and diffusion mechanisms

of nonlinear response, the local and nonlocal components of nonlinearity are very important. Absorption of interfering external and/or internal (generated in PRC) light fields leads to spatially nonuniform photogeneration of free carriers. Then, their drift in the external electric field and/or spatial diffusion follow. Resulting from further trapping of these carriers by defects and impurities (so-called traps), a spatially nonuniform distribution of internal electric field is formed. Under this conditions our mathematical model of propagation of the beams is,

$$\delta n = \beta |a|^2 + \gamma \frac{\partial |a|^2}{\partial X} \tag{2}$$

where $\beta = (1/2)k^2 a_0^2 n_0^4 r E_0$ is the Kerr coefficient; r is the linear electro-optic coefficient corresponding to this particular orientation of the PRC and polarization of the light; E_0 is the external electric field applied to the PRC in the transversal direction x ;

$$\mu = \frac{k_B T}{2e} k_0^2 \alpha_0 n_0^4 r$$

is the numerical constant characterizing the strength of the diffusion photorefractive nonlinearity (diffusion constant), T is the Boltzmann temperature constant; e is the electron charge. The coefficient of diffusion is

$$\gamma = \frac{\mu}{\beta} = \frac{k_B}{e a_0 E_0} = 2.5 \times 10^{-2} \frac{1}{E_0 a_0} \ll 1.$$

The sign of γ depends on the external electric field applied E_0 ; substituting Eq.(2) in Eq.(1) we obtain,

$$i \frac{\partial a}{\partial Z} = \frac{1}{2} \frac{\partial^2 a}{\partial X^2} + \beta |a|^2 + \gamma \frac{\partial |a|^2}{\partial X}. \tag{3}$$

The detailed discussion about the stable solutions in PRC with drift and diffusion, was made by V. Aleshkevich *et al.* [30]. Asymmetric soliton type solutions are stable, whereas multi-soliton solutions are unstable due to the perturbations sensibility.

For our case, we are interested in spatial solitons reflected by a nonlinear interface (with drift and diffusion nonlinearities governed in PRC), and a second linear media (air). Using the abrupt change of the refractive index between nonlinear-linear media[3,21], it is possible to obtain,

$$i \frac{\partial a}{\partial Z} = \frac{1}{2} \frac{\partial^2 a}{\partial X^2} + f(X) \left(\Delta + \beta |a|^2 + \gamma \frac{\partial |a|^2}{\partial X} \right) a, \tag{4}$$

where $\Delta = (n_{01} - n_{02}) / \bar{n}_2 |a_0|^2$; $f(X) = U(X)$; $U(X) = 1$ if $X \leq 0$ and $U(X) = 0$ if $X > 0$; $f(X) = (1/2)[1 - \tanh(\kappa x)]$ to describe general interface; κ represents the steepness of the interface. Note if $\gamma = 0$ and $\beta = 1$, the solution is, $a(X, Z) = \text{sech}(X) \exp[-iZ/2]$. However, if the diffusion and drift mechanism are taken together, then the solutions can be numerically studied. In the next section we extend a discussion of the numerical results.

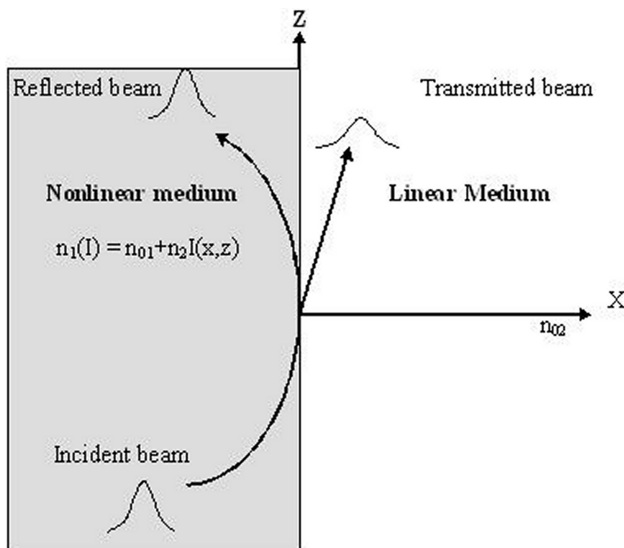


FIGURE 1. Scheme of the interface formed by nonlinear and linear medium.

3. Numerical solutions

We use a numerical split-step method [31] to solve Eq.(6). The initial condition is,

$$a(X, Z = 0) = A \operatorname{sech}(X - X_0) \exp(-iZ + \phi) \quad (5)$$

where A is the amplitude of the beam, X_0 is the initial position before propagation. Figure 2 shows very interesting propagation phenomena of a spatial soliton for saturation coefficient value of $\gamma = 0.2$. Unlike of total internal reflection with incident angle, this is not necessary for self-bending effect. The spatial soliton is supported by drift nonlinearity; in the same figure the spatial soliton is reflected by nonlinear interface but, newly the soliton is launched to nonlinear interface due to diffusion nonlinearity, and so on. As a consequence, spatial undulatory soliton is propagated with constant energy along its trajectory. Now the question is: what happens if the diffusion coefficient is increased? Figure 3 represents this case. The beam is launched more easily to nonlinear interface, and the beam is splitted in linear and nonlinear mediums. The reflected beam is smaller than the incident beam and its form is conserved. The energy of the beam in the linear medium is diffracted. On the other hand, the mass center is a very important characteristic of the nonlinear interfaces, because with this parameter is possible to obtain information about the trajectory of the beam in the interface. The mass center is defined by [21],

$$\hat{x} \equiv \frac{\int_{-\infty}^{\infty} a^* X a dX}{\int_{-\infty}^{\infty} a a^* dX}. \quad (6)$$

The trajectory of the mass center, for different values of diffusion coefficient, is shown in Fig. 4. The picture shows

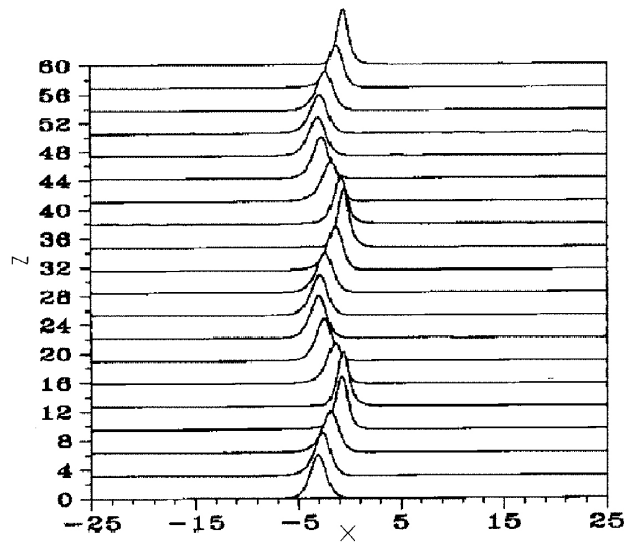


FIGURE 2. Undulatory behaviour of the spatial soliton propagated in a nonlinear interface. Drift and diffusion nonlinearities give periodic reflection and incidence with $\gamma = 0.2$.

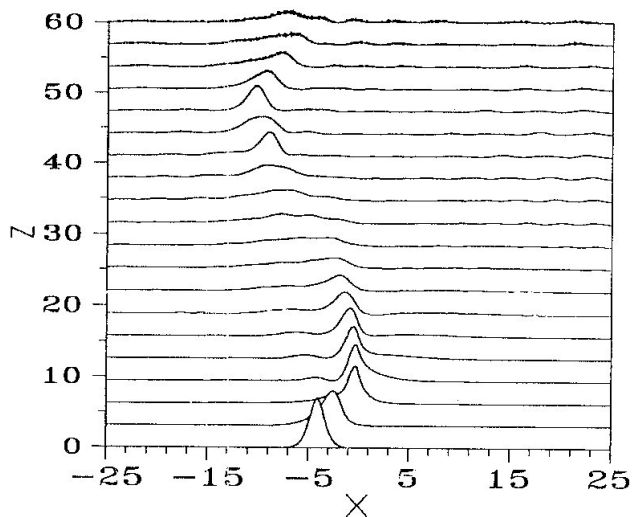


FIGURE 3. For $\gamma = 0.8$ the undulatory surface soliton loses its energy by diffraction in linear medium.

the behaviour of the beam during propagation. Observe the undulatory trajectory of the beam in the nonlinear medium. If we increase the diffusion coefficient, the trajectory is asymmetric and not parabolic. This case is equivalent to increasing the incident angle of the beam, in consequence the increments are less. In this case, we do not observe the Goos-Hänchen shift reported for total internal reflection [3,21] due to diffusion nonlinearity.

Figure 5 shows the variations of maximum intensity of the beam along the distance of propagation. If the diffusion coefficient parameter is increased, the oscillations increase, as a consequence, the energy decreases; this case is represented in Fig. 6. Observe that the sum of the percentage of energy of the reflected beam and the transmitted beam, is not constant with respect to the initial beam, because part of the beam in the linear medium is lost by diffraction.

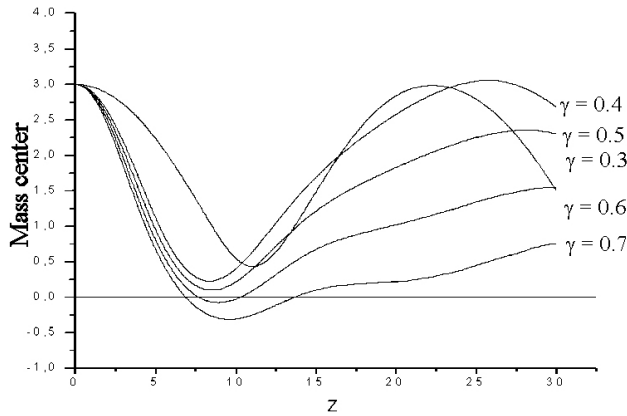


FIGURE 4. Mass center of the undulatory spatial solitons for different γ values.

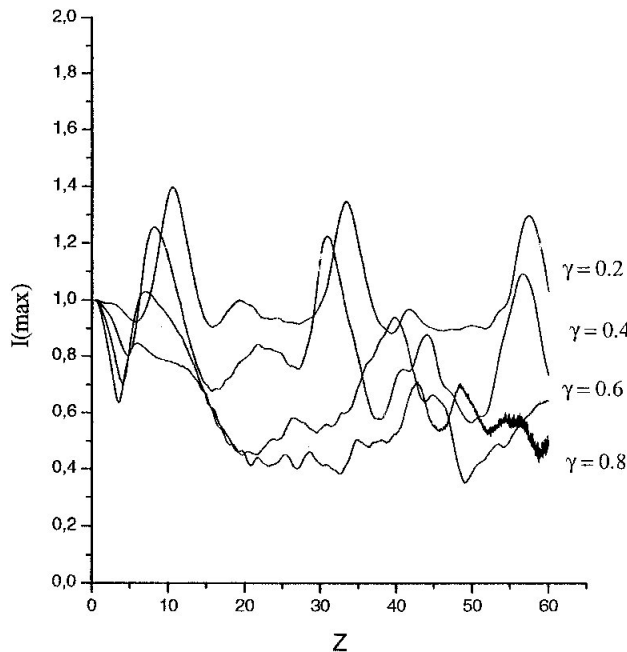


FIGURE 5. Maximum intensity of the undulatory surface soliton in function of the distance of propagation.

In the next section we describe the trajectory of the surface soliton with particle technique.

4. Dynamics of the undulatory soliton

We use the particle theory developed by Aceves *et al.* [20] to find the exact trajectory of the beam. According to this theory, the nonlinear interface characteristics can be obtained from the mass center dynamics. The nonlinear Schrödinger equation has been modified in our previous papers and has the form[3,21],

$$iP_0 \frac{d^2x}{dZ^2} = \frac{1}{2} \int (a \frac{\partial a^*}{\partial X} - a^* \frac{\partial a}{\partial X}) dX \quad (7)$$

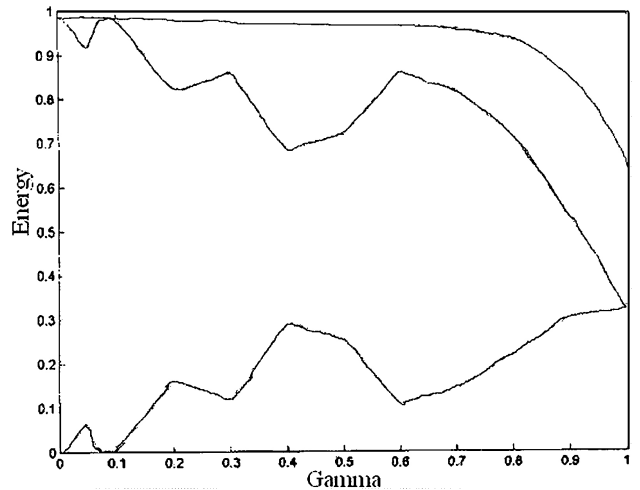


FIGURE 6. Energy of the undulatory surface soliton in function of the γ .

where $P_0 = \int aa^*dX$. If we differentiate Eq. (7) and use Eq. (3) we obtained,

$$P_0 \frac{d^2x}{dZ^2} = -\gamma \int_{-\infty}^{\infty} (\Delta \frac{\partial f(x)}{\partial X} |a|^2 + \frac{1}{2} \frac{\partial f(x)}{\partial X} |a|^4 + \mu f(x) (\frac{\partial |a|^2}{\partial X})^2) dX. \quad (8)$$

The Eq. (8) represents the influence of the repulsion from the dielectric-photorefractive crystal boundary on the beam trajectory. Further, within the frames of the method of the effective particles, we assume that the self-bending and the repulsion from the boundary do not affect strongly the stationary beam shape (this assumption is valid even when the laser beam reflects from the boundary at the angle close to the total internal reflection angle). This means that when obtaining the approximate beam center trajectory one can substitute, into the integral in the right part of Eq. (8) an approximate expression for $a(X, Z) = \text{sech}[\kappa(X - X_0(z))]$ (where κ is the form-factor), which is the solution of the standard unperturbed Schrödinger equation. Substituting in Eq. (10) it is possible to obtain,

$$\frac{d^2x}{dZ^2} = -\frac{1}{2} \Delta \kappa \text{sech}^2(\kappa X_0) - \frac{1}{4} \kappa^3 \text{sech}^4(\kappa X_0) + \frac{4}{15} \mu \kappa^4 + \frac{2}{5} \mu \kappa^4 [\text{sech}^4(\kappa X_0) - 1] \tanh(\kappa X_0) + \frac{2}{15} \mu \kappa^4 \tanh^3(\kappa X_0). \quad (9)$$

When $X_0 \rightarrow -\infty$ (that means that the beam goes away from the air-PRC boundary into the volume of PRC) the last equation transforms into that describing the beam self-bending along the parabolic trajectory in the PRC, and using boundary conditions, (X_0 and initial angle of incidence V_0 at $Z = 0$),

$$X(Z) = X_0 + V_0 Z + \frac{8}{15} \mu \kappa Z^2. \quad (10)$$

The Eq. (10) describes the parabolic trajectory of the beam spatial soliton during its propagation. Figure 7 shows

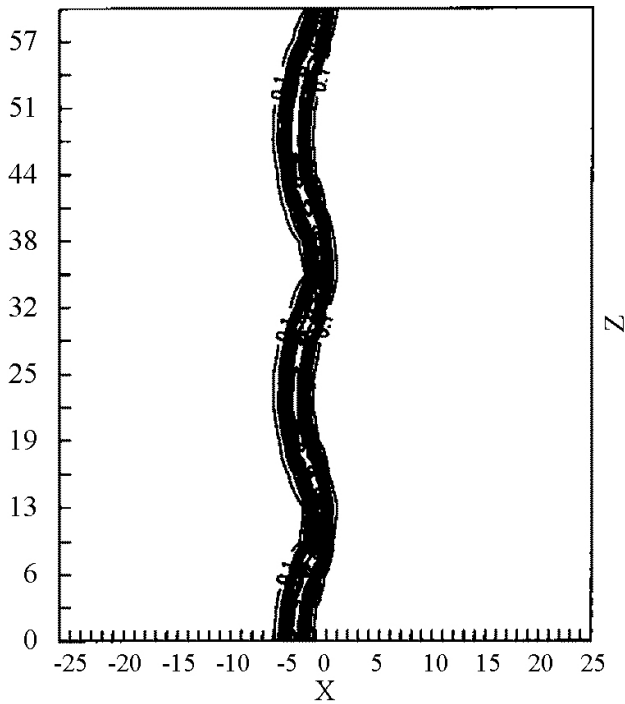


FIGURE 7. Parabolic trajectory of the surface soliton for $\gamma = 0.2$ value.

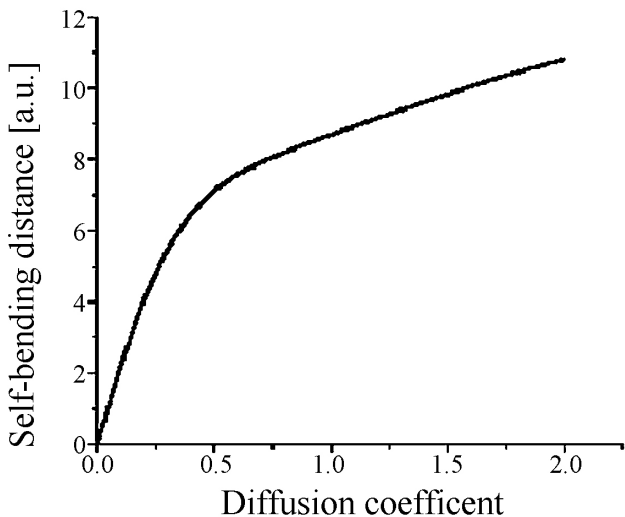


FIGURE 8. Dependence between bending distance vs. diffusion coefficient.

the trajectory of the beam for $\gamma = 0.2$, where it is possible to observe a reflection by the nonlinear interface, as a consequence, surface waves are formed in the nonlinear interface.

5. Experimental results vs. theoretical predictions

Experimental studies about self-bending beams in photorefractive crystals, were done by Petter *et al.* [28]. It is known

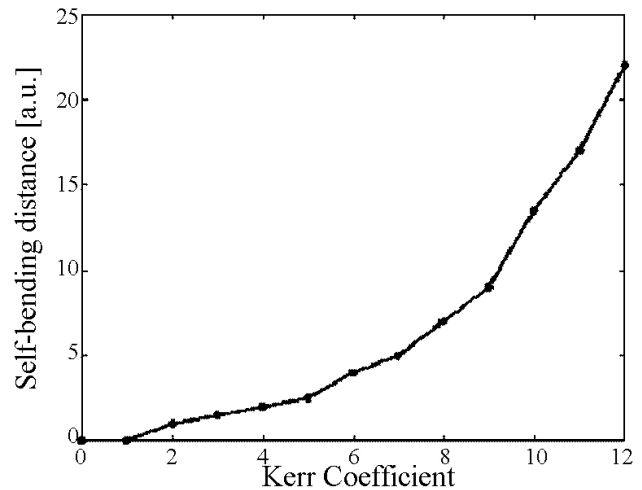


FIGURE 9. Dependence between bending distance vs. Kerr coefficient.

that self-bending of photorefractive solitons is caused by diffusion in photorefractive crystals, and becomes an important effect when the beam size is in the range of the diffusion length for the charge carriers. Figure 8 shows the numerical results of the examination of the bending distance in dependence with the diffusion coefficient. The decrease of the bending distance, at higher beam intensities (implicit in diffusion coefficient), is mainly due to the beam widening and therefore the smaller gradient for the saturated nonlinearity. The propagation distance was 20 diffraction length, and comparing our numerical data with that found experimentally we can see good qualitative agreement. Figure 9 shows the bending distance in dependence on the Kerr coefficient. In the range of higher saturation ($I_{\text{beam}}/I_{\text{output}} > 1$), the form of the curve is quadratic relation approximately. It also agrees with the experimental results of Petter *et al.*

6. Conclusions

We studied quasi-surface waves formed in a nonlinear interface by drift and diffusion nonlinearity mechanism. For $\gamma < 0.4$, surface waves are formed. For other values of γ the beam is splitted in two beams, and part of the beam in the linear medium is diffracted. Other important point, is that the trajectory of the beam along the boundary PRC-air interface shows a parabolic behaviour.

Acknowledgments

This work was supported by CONACyT, projects J32018-A, J35313-A, J35303-A, UG-E20391, and CONCyTEG-FONINV No. 5987. Support to the teacher's degree in Electric Engineering, in Instruments and Digital Systems.

- † In memory of our friend Gustavo E. Torres-Cisneros.
1. J. Scheuer and M. Orenstein, *Opt. Lett.* **24** (1999) 1735.
 2. Yu. S. Kivshar, A.M. Kosevich, and O.A. Chubykalo, *Phys. Rev. A* **41** (1990) 1677.
 3. E. Alvarado-Méndez, G.E. Torres-Cisneros, M. Torres-Cisneros, J.J. Sánchez-Mondragón, and V. Vysloukh, *Opt. and Quant. Elect.* **30** (1998) 687.
 4. B. Crosignani *et al.*, *J. Os. Opt. Soc. Am. B* **10** (1993) 446.
 5. G. Duree *et al.*, *Phys. Rev. Lett.* **74** (1995) 1978.
 6. M. D. Iturbe-Castillo, P. Márquez-Aguilar, J. Sánchez-Mondragón, S. Stepanov, and V. Vysloukh, *Appl. Phys. Lett.* **64** (1994) 408.
 7. D. Christodoulides and M. Carvalho, *J. Opt. Soc. Am. B* **12** (1995) 1628.
 8. Z. Chen *et al.*, *Opt. Lett.* **21** (1996) 1821.
 9. Z. Chen, M. Seguev, T. Coskun, and D. Christodoulides, *J. Opt. Soc. Am. B* **14** (1997) 1407.
 10. A. Zozulya, D. Anderson, A. Mamaev, and M. Saffman, *Phys. Rev. A* **57** (1998) 522.
 11. S. Bian, J. Frejlich, and K. Ringhofer, *Phys. Rev. Lett.* **78** (1997) 4035.
 12. G. García-Quirino, M. D. Iturbe-Castillo, V. Vysloukh, and S. Stepanov, *Opt. Lett.* **22** (1997) 154.
 13. W. Krolikowski, B. Luther-Davies, C. Denz, and T. Tschudi, *Opt. Lett.* **23** (1998) 97.
 14. W. Krolikowski and S. Holmstrom, *Opt. Lett.* **22** (1997) 369.
 15. A. Mamaev, M. Saffman, and A. Zozulya, *J. Opt. Soc. Am. B* **15** (1998) 2079.
 16. J.A. Andrade-Lucio *et al.*, *Elect. Lett.* **36** (2000) 1403.
 17. E. Ostrovskaya and Y. Kivshar, *Opt. Lett.* **23** (1998) 1268.
 18. W. Krolokowski, M. Saffman, B. Luther-Davies, and C. Denz, *Phys. Rev. Lett.* **80** (1998) 3240.
 19. I.V. Shadrivov and A. Zarov, *J. Opt. Soc. Am. B* **19** (2002) 596.
 20. A.B. Aceves, J.V. Moloney, and A.C. Newell, *Phys. Rev. A I* **39** (1989) 1809; *Phys. Rev. A II* **39** (1989) 1828.
 21. E. Alvarado-Méndez *et al.*, *Opt. Comm.* **193** (2001) 267.
 22. H. Gilles, S. Girard, and J. Hamel, *Opt. Lett.* **27** (2002) 1421.
 23. D.N. Christodoulides and M.I. Carvalho, *Opt. Lett.* **19** (1994) 1714.
 24. M.I. Carvalho, S.R. Singh, and D.N. Christodoulides, *Opt. Comm.* **120** (1995) 311.
 25. M. Seguev, G.C. Valley, B. Crosigniani, P. Diporto, and A. Yariv, *Phys. Rev. Lett.* **73** (1994) 3211.
 26. D.N. Christodoulides and M.I. Carvalho, *J. Opt. Soc. Am. B.* **12** (1995) 1628.
 27. M.F. Shih, P. Leach, and M. Seguev, *Opt. Lett.* **21** (1996) 324.
 28. J. Petter, C. Weilnau, C. Denz, A. Stepken, and F. Kaiser, *Opt. Comm.* **170** (1999) 291.
 29. G.S. García-Quirino, J.J. Sánchez-Mondragón, and S. Stepanov, *Phys. Rev. A* **51** (1995) 1571.
 30. V. Aleshkevich, Y. Kartashov, and V. Vysloukh, *Physical Rev. E* **63** (2000) 016603.
 31. G.P. Agrawal, *Nonlinear Fiber Optics*, (academic Press, 1989) p. 44.